# Measurement of Sound Velocity in a Fermi Gas near a Feshbach Resonance

J. Joseph, B. Clancy, L. Luo, J. Kinast, A. Turlapov, and J. E. Thomas*

*Department of Physics, Duke University, Durham, North Carolina, 27708, USA*

(Received 21 December 2006; published 24 April 2007)

Sound waves are excited in an optically trapped degenerate Fermi gas of spin-up and spin-down atoms with magnetically tunable interactions. Measurements are made throughout the crossover region, from a weakly interacting Fermi gas through the resonant Fermi superfluid regime to a Bose condensate of dimer molecules. The measured sound velocities test theories of hydrodynamic wave propagation and predictions of the equation of state. At resonance, the sound velocity exhibits universal scaling with the Fermi velocity, to within 1.8% over a factor of 30 in density.

DOI: 10.1103/PhysRevLett.98.170401 PACS numbers: 03.75.Ss, 32.80.Pj

Optically trapped, strongly interacting Fermi gases [1] provide a unique laboratory for testing nonperturbative many-body theories in a variety of fields, from neutron stars and nuclear matter [2] to quark-gluon plasmas [3] and high temperature superconductors [4]. In contrast to these other systems, interactions in ultracold atomic Fermi gases are magnetically tunable using a Feshbach resonance [5]. At magnetic fields well above the resonance, one obtains a weakly attractive Fermi gas, while well below the resonance, spin-up and spin-down atoms are joined into dimer molecules, which form a Bose-Einstein condensate (BEC) [6–9]. Near resonance, the gas is a strongly interacting Fermi superfluid [10].

In this Letter, we report a precision test of hydrodynamic models of sound propagation throughout the resonance region [11–13] and of predictions of the equation of state [14–17] $\mu_{\rm loc}(n)$, where $\mu_{\rm loc}$ is the local chemical potential per atom and $n$ is the total density of atoms. Existing measurements of release energy [9], momentum distribution [18], and cloud size [19] could also be used for testing $\mu_{\rm loc}(n)$. Precise interpretation of these measurements, however, would depend on microscopic models. Connecting the release energy to $\mu_{\rm loc}(n)$ requires knowledge of $\mu_{\rm loc}(n)$. Measurements of momentum distributions depend on the dynamics of magnetic sweeps [20], which turn off the interactions. Cloud size measurements are sensitive to the state of the gas at the edges, which at finite temperatures may differ from the superfluid core [21] that is probed in sound speed measurements. Model-independent measurements of collective breathing mode frequencies [22–25] probe only the density scaling of $\mu_{\rm loc}(n)$, i.e., the polytropic index $\gamma = \partial \ln \mu_{\rm loc}(n)/\partial \ln n$ and not the magnitude of $\mu_{\rm loc}(n)$. As a result, in the universal regime, theories with different ground states predict identical breathing mode frequencies [26,27], but different sound speeds.

The medium for the sound propagation is a 50:50 mixture of $^6$Li atoms in the two lowest internal states or a BEC of $Li_2$ molecules near a broad Feshbach resonance centered at $B = 834$ G [28]. The gas is cooled by forced evaporation in an ultrastable $CO_2$ laser trap at the resonant magnetic field [1]. Near the end of evaporation, $B$ is adiabatically set to a chosen final value between 700 and 1100 G, and the trap is adiabatically recompressed to a desired depth $U_0$ between 0.14 and 80 $\mu$K.

The samples are nearly in the many-body ground state of the trapped atoms, as indicated by the cloud spatial profiles: We observe a zero-temperature Thomas-Fermi shape close to the Feshbach resonance, as expected for a unitary gas at zero temperature [29]; in the molecular BEC regime, we do not observe a thermal component. At zero temperature, the dimensionless interaction parameter $1/k_F a$ is the only quantity that determines the physics. We tune the Fermi wave vector $k_F$ by varying $U_0$ to change the sample density. The $s$-wave scattering length $a = a(B)$ is varied by changing the magnetic field and is estimated from Ref. [28]. At $|k_F a| \gg 1$ the system is in the strongly interacting regime and is a superfluid. The BEC (weakly interacting Fermi) regime corresponds to $1/k_F a > 1$ ($1/k_F a < -1$).

A sound wave is excited by a method similar to that used for a BEC of atoms [30]. A green 532 nm laser beam passes through a cylindrical telescope to create a knifelike elliptical beam (half widths at $1/e$, 15 $\mu$m by 150 $\mu$m) which bisects the long axis of the cigar-shaped atom cloud; Fig. 1 (top). A repulsive knife potential arises from the blue detuning of the 532 nm beam (671 nm Li transition), with a maximum height $U_{\rm knife}$ between 0.5 and 14 $\mu$K, as determined from the atomic polarizability and the 532 nm beam area and power. The knife is pulsed on for 280 $\mu$s, much shorter than the sound propagation times $\sim$10 ms, creating a density perturbation which propagates along the axial coordinate $z$ for a chosen hold time. Then the cloud is released and expands, after which it is destructively imaged for 5 $\mu$s with a spatial resolution (for the entire imaging system) of 5.5 $\mu$m [22]. Figure 1 (bottom) shows the perturbed density profile and the difference between the perturbed and unperturbed profiles for several propagation times. Peaks (valleys) are located in the difference signal by setting all negative (positive) values to

 

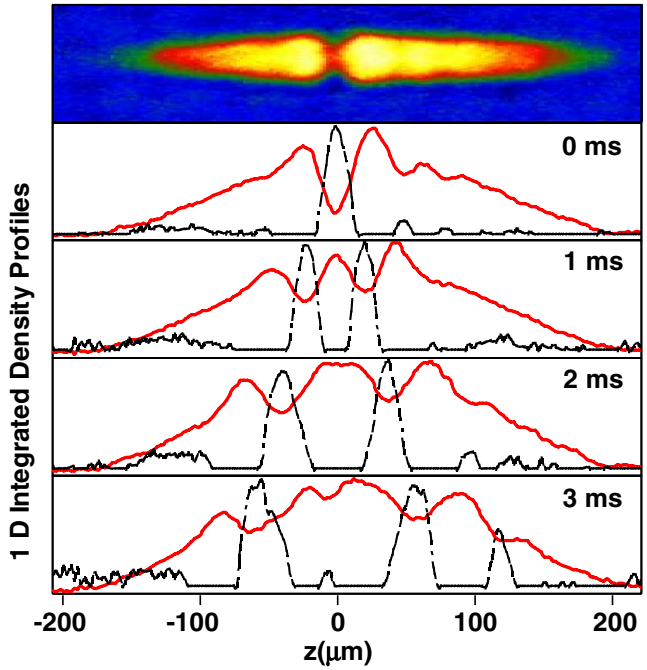


FIG. 1 (color online). Sound propagation at the Feshbach resonance: (Top) 2D density profile showing initial perturbation. (Bottom) Gray (red) solid curve: Axial density profiles of the cloud for different in-trap propagation times; black dashed curve: valleys (inverted).

zero. Fitting a shifted Gaussian to each feature yields its position as a function of propagation time.

The main result of this Letter, Fig. 2, is the measurement of $c_0/v_F$, the normalized sound velocity in the center plane (at $z = 0$) versus $1/k_F a$. The reference Fermi velocity $v_F$ and $k_F$ are those of a noninteracting Fermi gas, i.e., $E_F = \hbar(\omega_x\omega_y\omega_z)^{1/3}(3N)^{1/3} = m_{\mathrm{atom}}v_F^2/2 = \hbar^2k_F^2/2m_{\mathrm{atom}}$, where $E_F$ is the Fermi energy. Data are corrected for systematics. Error bars in $c_0/v_F$ and $1/k_F a$ are statistical (see below).

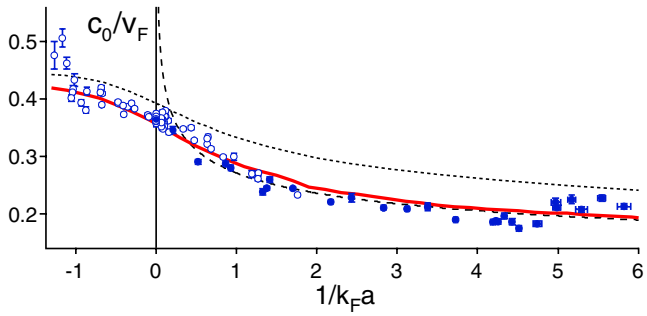


FIG. 2 (color online). Normalized sound velocity $c_0/v_F$ versus the interaction parameter, $1/k_F a$. Black dotted curve: mean-field theory based on the Leggett ground state [33]. Gray (red) solid curve: quantum Monte Carlo calculation [33]. Black dashed curve: Thomas-Fermi theory of a molecular BEC, using $a_{\mathrm{mol}} = 0.6a$. Closed and open circles represent trap depths 140–500 nK and 0.6–80 $\mu$K, respectively.

We determine $v_F$ by characterizing the trap frequencies and atom number. The trap frequencies $\omega_i$ are calibrated for each velocity measurement. The mean radial frequency $\omega_\perp = \sqrt{\omega_x\omega_y}$ is calculated from the radial breathing mode frequency $\omega_{\mathrm{breath}}$ [22,24]. $\omega_{\mathrm{breath}}$ is measured either at resonance, using $\omega_{\mathrm{breath}} = \sqrt{10/3}\omega_\perp$, or in the far BEC regime, where we assume $\omega_{\mathrm{breath}} = 2\omega_\perp$ neglecting a small beyond-mean-field correction [25,27]. The ratio $\omega_x/\omega_y = 1.056$ and the axial frequency $\omega_z$ are measured using parametric resonance in a weakly interacting Fermi gas [22]. The frequency of the magnetic field potential, $\omega_B/2\pi = 20.5$ Hz at 834 G, is measured using a sloshing mode. The trap anisotropy ratio $\omega_\perp/\omega_z$ is between 4.1 and 25 depending on $U_0$. For $U_0 = 8.3$ $\mu$K, $\omega_\perp/2\pi = 688(2)$ Hz and $\omega_z/2\pi = 34.4(0.2)$ Hz. All radial frequencies have been corrected for anharmonicity [22,24].

The total number of atoms $N$ is determined from the column density $\tilde{n}$. We employ high field resonant absorption imaging using a 5 $\mu$s pulse on a two-level cycling transition [22]. The calculated $\tilde{n}$ includes imperfect polarization and a finite saturation parameter. $N$ varies from $6 \times 10^4$ for a molecular BEC to $5 \times 10^5$ near and above resonance. We correct for laser frequency fluctuations, which reduces the measured value of $N$ relative to the true value. After correction, the statistical standard error in the mean $N$ is $<6\%$, 2% on average.

Five additional measures are taken to reduce systematic errors. First, by tracking both right- and left-propagating features (Fig. 3) we eliminate effects due to the overall motion of the cloud. Second, we correct for a small change in the axial cloud size between release and imaging: The measured in-trap positions of the propagating features are scaled by a hydrodynamic expansion coefficient [1,31]. The correction is $<4.7\%$, 1.2% on average.

Third, we account for the dependence of the velocity on the nonuniform density distribution along $z$. Making a general approximation for the equation of state $\mu_{\mathrm{loc}}(n) = Cn^\gamma$ and calculating the velocity using hydrodynamic theory [12,13], one finds that $c(z) \propto \sqrt{1 - z^2/R_z^2}$

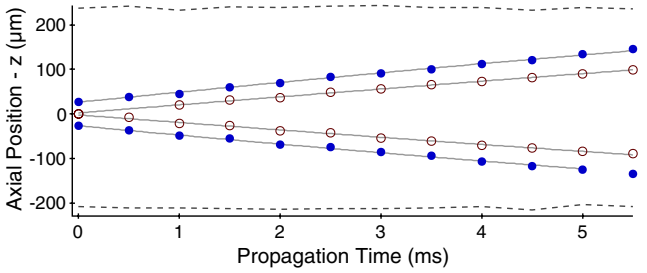


FIG. 3 (color online). Axial positions $z$ of the left- and right-traveling density features of Fig. 1 versus the in-trap propagation time. Coordinates of the valleys [closed (blue) circles] and front peaks [open (red) circles] are shown. Dashed lines correspond to the measured Fermi radii ($z = \pm R_z$).

for a harmonically trapped gas, where $R_z$ is the axial Thomas-Fermi radius. Then, a small density perturbation propagates as $z(t) = R_z \sin(\pm c_0 t/R_z + \varphi)$, where $\varphi = \arcsin(z_{\text{knife}}/R_z)$, with $z_{\text{knife}}$ the excitation position. $c_0$, the velocity of the features at $z = 0$, is obtained by fitting the coordinates of the propagating features which lie within the central 65% of the cloud; Fig. 3. The statistical error in $c_0$ from the fit is found to be <5.3%, 1.3% on average.

Fourth, we account for nonlinearity in propagation: The front peak moves faster than the valley, as predicted earlier for BECs [32]. In Fig. 4, we show the velocities of the valley and peak versus the excitation strength, $U_{\text{knife}}/\mu$, where $\mu$ is the global chemical potential estimated using Monte Carlo modeling [15,33]. The peak and valley velocities vary with excitation strength, but the mean velocity remains constant. All velocities converge to a single value at low excitation strength showing that the reported mean accurately represents the velocity of an infinitesimal perturbation. For the data of Fig. 2, $U_{\text{knife}}/\mu$ ranges from 1 to 30. We do not observe formation of shock waves which are predicted for a BEC [32].

Fifth, the sound velocity data are corrected for anharmonicity of the trapping potential. For shallow traps, where the correction is greatest, the axial potential is primarily magnetic and harmonic, while the radial confinement is optical and Gaussian. The corrections for $c_0$ are calculated to first order in $\mu/U_0$ using Eq. (1). For $1/k_F a \leq 0$, we use a Fermi equation of state ($\gamma = 2/3$) and obtain $c_0/c_0^{\text{meas}} = 1 + 0.10\mu/U_0$. For $1/k_F a > 1$, we assume a molecular BEC ($\gamma = 1$) and obtain $c_0/c_0^{\text{meas}} = 1 + 0.14\mu/U_0$. For $0 < 1/k_F a < 1$, these two corrections are linearly combined. $\mu/U_0$ ranges from 0.025 to 0.43. The net anharmonic correction to $c_0/v_F$ is <2.5%, 0.5% on average.

Linking the measured speed of sound $c_0$ to the equation of state $\mu_{\text{loc}}(n)$ enables quantitative tests of theories. By analyzing the wave front shape, we find that the hydrodynamic model of Capuzzi *et al.* [12], for a cigar-shaped trap, provides a correct description of the propagation. The primary result of this model is that the wave front speed is independent of $x$, $y$, i.e., $c(x, y, z) = c(z)$, where

$$c(z) = \left(\frac{1}{m_{\text{atom}}} \frac{\int n dx dy}{\int (\partial \mu_{\text{loc}}/\partial n)^{-1} dx dy}\right)^{1/2}. \qquad (1)$$

In contrast, a simple model of isotropic sound propagation assumes $c_{\text{loc}}(n) = \sqrt{n(\partial \mu_{\text{loc}}/\partial n)/m_{\text{atom}}}$. For the same equation of state, the trap-averaged value of $c_{\text{loc}}(n)$ differs from Eq. (1) by a few percent. However, the predicted line of sight $y$ integrated $c_{\text{loc}}(n)$ depends on $x$ [Fig. 5 (dashed curve)], while the measured speed is independent of $x$. This validates Eq. (1) for our experimental conditions, enabling comparison of Fig. 2 data to theory.

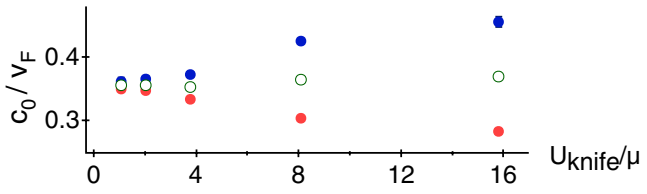


FIG. 4 (color online). Valley [light gray (red) closed circles], peak [dark gray (blue) closed circles], and mean [open (green) circles] velocity versus excitation potential normalized to the global chemical potential. Measured at the Feshbach resonance.

In the BEC regime, at $1/k_F a > 1$, the experiment tests the interaction properties of composite bosons, molecules made out of two fermions. One may approximate the state of the gas as a BEC of singlet molecules that collides with $s$-wave scattering length $a_{\text{mol}}$. Using the local equation of state $\mu_{\text{loc}}(n) = \mu_{\text{mol}}(n)/2 = \pi\hbar^2 a_{\text{mol}} n/m_{\text{mol}}$ in Eq. (1), one finds $c_0/v_F = (5/2k_F a_{\text{mol}})^{1/5}/4$. An exact solution of the four-fermion scattering problem predicts $a_{\text{mol}} = 0.6a$ [34] and a speed in good agreement with the measurements (black dashed curve in Fig. 2). In contrast, the Leggett ground state predicts $a_{\text{mol}} = 2a(B)$ and a 27% higher speed in the BEC regime [35].

Our data tests predictions of the equation of state for the entire crossover from Fermi to Bose regimes; Fig. 2. The black dotted curve [33] represents a Leggett ground state approximation [35], which predicts significantly higher speed than measured except on the Fermi side of the resonance. The red solid curve [33] shows the Monte Carlo result [15], which is in much better agreement with the data. Interestingly, in most of the molecular BEC regime, for $1/k_F a > 1$, the data are systematically lower than the prediction.

The lower measured speed in the BEC regime, $1 < 1/k_F a < 5$, may arise from the coupling of first and second sound, the latter of which travels slower [11]. However, high temperature does not seem a likely cause, as we observe no thermal component. At resonance, we also observe increased velocity when we significantly increase the energy of the gas. The lower speed probably does not arise from a dark soliton, which travels slower than sound.

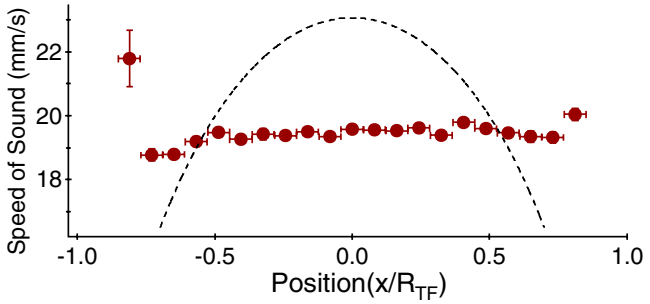


FIG. 5 (color online). Local sound velocity at the Feshbach resonance versus transverse coordinate $x$, showing a flat wave front. $x$ is given in units of the Thomas-Fermi radius. Images were divided into 21 longitudinal segments of equal transverse width. For the $i$th segment, $c_i(z = 0)$ is measured. The dashed curve represents the line of site averaged isotropic sound speed, showing curved wave front.

Solitons are comparable in size to the coherence length [36,37], $\hbar/\sqrt{2\mu m_{\rm mol}} < 1\ \mu$m, and maintain shape in propagation, while the observed density depressions are 10–20 $\mu$m wide and spread.

On the far Fermi side of the Feshbach resonance, at $1/k_F a < -1.3$, propagation of sound is not observed. Instead, the hole from the laser knife fills without propagating, as in a noninteracting gas. At the temperatures we achieve, the gas is not necessarily a superfluid in the weakly interacting Fermi gas region, and hydrodynamic sound propagation is provided by collisional, rather than superfluid, hydrodynamics.

We also attempted to measure the sound velocity as far into the weakly interacting molecular BEC regime as possible. To achieve $1/k_F a > 5$, the trap depth and magnetic field were tuned to minimize $k_F$ and $a$ simultaneously, and $c_0/v_F$ appears to increase. In this case, however, after release, the chemical potential was not large enough compared to the remaining magnetic trapping potential to obtain adequate expansion for ideal absorption imaging.

The universal hypothesis is positively tested in our measurements. The hypothesis states that $c_0/v_F$ should be independent of density when $k_F a = \infty$, provided that the effective range of the interaction potential is small compared to the interparticle spacing [2]. Indeed, at resonance, 834(2) G, we observe that $c_0/v_F$ remains constant to 1.8% as the trap depth is changed from 410 nK to 80 $\mu$K, i.e., a factor 30 in density. In contrast, below the Feshbach resonance, at 821 G, $c_0/v_F$ decreases with decreasing $U_0$. These measurements of $c_0/v_F$ vs $U_0$ also show that the Feshbach resonance location is much closer to 834 G [28] than to 822 G [9,38].

From the sound velocity at resonance, we have also measured the universal constant $\beta$ [1,2], which connects the local Fermi energy of a noninteracting gas $\epsilon_F(n) = (3\pi^2 n)^{2/3}\hbar^2/2m_{\rm atom}$ to that of a strongly interacting gas in the universal regime: $\mu_{\rm loc}(n) = (1+\beta)\epsilon_F(n)$. Using Eq. (1), we obtain

$$\frac{c_0}{v_F} = \frac{(1+\beta)^{1/4}}{\sqrt{5}}, \qquad (2)$$

from which we find $\beta = -0.565(0.015)$, after correction for the systematic errors described above. The remaining statistical error includes contributions from $v_F$ ($N$, trap frequencies), magnetic field, and $c_0$.

We thank G. Astrakharchik, P. Capuzzi, L. Carr, K. Levin, Qijin Chen, Yan He, K. Machida, and T. Ghosh for stimulating discussions and correspondence. This research was supported by ARO, NSF, DOE, and NASA.

*Electronic address: jet@phy.duke.edu

[1] K. M. O'Hara *et al.*, Science **298**, 2179 (2002).
[2] H. Heiselberg, Phys. Rev. A **63**, 043606 (2001).
[3] P. F. Kolb and U. Heinz, *Quark Gluon Plasma 3* (World Scientific, Singapore, 2003), p. 634.
[4] Q. Chen *et al.*, Phys. Rep. **412**, 1 (2005).
[5] M. Houbiers *et al.*, Phys. Rev. A **57**, R1497 (1998).
[6] S. Jochim *et al.*, Science **302**, 2101 (2003).
[7] M. Greiner, C. A. Regal, and D. S. Jin, Nature (London) **426**, 537 (2003).
[8] M. W. Zwierlein *et al.*, Phys. Rev. Lett. **91**, 250401 (2003).
[9] T. Bourdel *et al.*, Phys. Rev. Lett. **93**, 050401 (2004).
[10] M. Zwierlein *et al.*, Nature (London) **435**, 1047 (2005).
[11] H. Heiselberg, Phys. Rev. A **73**, 013607 (2006).
[12] P. Capuzzi *et al.*, Phys. Rev. A **73**, 021603(R) (2006).
[13] T. K. Ghosh and K. Machida, Phys. Rev. A **73**, 013613 (2006).
[14] A. Perali, P. Pieri, and G. C. Strinati, Phys. Rev. Lett. **93**, 100404 (2004).
[15] G. E. Astrakharchik *et al.*, Phys. Rev. Lett. **93**, 200404 (2004).
[16] A. Bulgac and G. F. Bertsch, Phys. Rev. Lett. **94**, 070401 (2005).
[17] N. Manini and L. Salasnich, Phys. Rev. A **71**, 033625 (2005).
[18] C. A. Regal *et al.*, Phys. Rev. Lett. **95**, 250404 (2005).
[19] M. Bartenstein *et al.*, Phys. Rev. Lett. **92**, 120401 (2004).
[20] M. L. Chiofalo, S. Giorgini, and M. Holland, Phys. Rev. Lett. **97**, 070404 (2006).
[21] J. Stajic, Q. Chen, and K. Levin, Phys. Rev. Lett. **94**, 060401 (2005).
[22] J. Kinast *et al.*, Phys. Rev. Lett. **92**, 150402 (2004).
[23] M. Bartenstein *et al.*, Phys. Rev. Lett. **92**, 203201 (2004).
[24] J. Kinast, A. Turlapov, and J. E. Thomas, Phys. Rev. A **70**, 051401(R) (2004).
[25] A. Altmeyer *et al.*, Phys. Rev. Lett. **98**, 040401 (2007).
[26] H. Hu *et al.*, Phys. Rev. Lett. **93**, 190403 (2004).
[27] G. E. Astrakharchik *et al.*, Phys. Rev. Lett. **95**, 030404 (2005).
[28] M. Bartenstein *et al.*, Phys. Rev. Lett. **94**, 103201 (2005).
[29] J. Kinast *et al.*, Science **307**, 1296 (2005).
[30] M. R. Andrews *et al.*, Phys. Rev. Lett. **79**, 553 (1997).
[31] C. Menotti, P. Pedri, and S. Stringari, Phys. Rev. Lett. **89**, 250402 (2002).
[32] B. Damski, Phys. Rev. A **69**, 043610 (2004).
[33] G. Astrakharchik (private communication).
[34] D. S. Petrov, C. Salomon, and G. V. Shlyapnikov, Phys. Rev. Lett. **93**, 090404 (2004).
[35] P. Nozières and S. Schmitt-Rink, J. Low Temp. Phys. **59**, 195 (1985).
[36] A. Jackson, G. M. Kavoulakis, and C. J. Pethick, Phys. Rev. A **58**, 2417 (1998).
[37] S. Burger *et al.*, Phys. Rev. Lett. **83**, 5198 (1999).
[38] C. H. Schunck *et al.*, Phys. Rev. A **71**, 045601 (2005).